Berberine and palmatine inhibit the growth of human rhabdomyosarcoma cells

Sayaka Shinji[a*], Shunichi Nakamura[a*], Yuma Nihashi[b], Koji Umezawa[c] and Tomohide Takaya[a,b,c]

[a]*Department of Agriculture, Graduate School of Science and Technology, Shinshu University, Nagano, Japan;*

[b]*Department of Science and Technology, Graduate School of Medicine, Science and Technology, Shinshu University, Nagano, Japan;*

[c]*Department of Biomolecular Innovation, Institute for Biomedical Sciences, Shinshu University, Nagano, Japan*

[*]These authors equally contributed to this work

Corresponding author: Tomohide Takaya. Department of Agriculture, Graduate School of Science and Technology, Shinshu University, 8304 Minami-minowa, Kami-ina, Nagano 399-4598, Japan

E-mail address: ttakaya@shinshu-u.ac.jp

Abbreviations: ARMS, alveolar rhabdomyosarcoma; ERMS, embryonal rhabdomyosarcoma; RMS, rhabdomyosarcoma

Abstract

A natural isoquinoline alkaloid, berberine, has been known to exhibit anti-tumor activity in various cancer cells *via* inducing cell cycle arrest. However, it has not been investigated whether berberine and its analogs inhibit the growth of rhabdomyosarcoma (RMS), which is the most frequent soft tissue tumor in children. The present study examined the anti-tumor effects of berberine and palmatine on expansions of three human embryonal RMS cell lines; ERMS1, KYM1, and RD. Intracellular incorporation of berberine was relatively higher than that of palmatine in every RMS cell line. Berberine significantly inhibited the cell cycle of all RMS cells at G_1 phase. On the other hand, palmatine only suppressed the growth of RD cells. Both of berberine and palmatine strongly inhibited the growth of tumorsphere of RD cells in three-dimensional culture. These results indicate that berberine derivatives have the potential of anti-tumor drugs for RMS therapy.

Keywords: berberine; palmatine; rhabdomyosarcoma; three-dimensional culture; tumorsphere

Introduction

An isoquinoline alkaloid, berberine, is abundantly involved in several medicinal plants, such as *Phellodendron amurense*, which has been used as a traditional Chinese herb. Besides berberine, these plants synthesize a series of protoberberine-type alkaloids, such as palmatine, coptisine, and jatrorrhizine (Figure 1(a)). Numerous studies have reported that berberine derivatives have a wide range of bioactivities including anti-bacterial, anti-diabetic, anti-inflammatory, anti-oxidative, cardiovascular protective, and neuroprotective effects [1]. Especially, the anti-tumor activities of berberine have been shown because it potentially overcomes drug resistance in combination with clinical chemotherapy [2]. Berberine induces cell cycle arrests or apoptosis of prostate carcinoma [3], bladder cancer [4], lung tumor [5], colon cancer [6], and hepatoma [7]. Berberine has been reported to arrest cell cycle not only in cancers but also in sarcomas, such as osteosarcoma [8] and chondrosarcoma [9]. However, the effects of berberine and its analogs on rhabdomyosarcoma (RMS) have not been studied yet.

RMS is the most frequent soft tissue tumor in children but rarely develops in adults. RMS is formed in soft tissues including striated muscles, and is considered to be derived from several muscular lineages, such as mesenchymal stem cells, myogenic precursor cells, or myoblasts [10]. RMS is classified into two subtypes, alveolar RMS (ARMS) and embryonal RMS (ERMS). ARMS is malignant and mostly occurs in the extremities of adolescents and young adults. 80% of ARMS has the chromosomal

translocation t(2;13)(q35;q14) or t(1;13)(p36;q14), which generates chimeric gene *PAX3-FOXO1* or *PAX7-FOXO1*, respectively [10-12]. Therefore, gene therapy is considered to be a relevant strategy for ARMS. However, around 70% of childhood RMS is ERMS, which has a variety of chromosomal abnormalities and can arise from every stage of muscle development [13]. At present, a combination of chemotherapy, surgery, and/or radiation has become the standard treatment for RMS. Although the 5-year survival rate of RMS has increased up to 60% in the 2000s [14], the oncological outcome of RMS patients has not been conspicuously improved in recent years because of drug resistance and metastatic diseases [10]. Development of effective and safe agents for RMS therapy is thus urgently required.

The present study investigated the inhibitory actions of berberine and palmatine on the growth of three ERMS cell lines, ERMS1, KYM1, and RD (Figure 1(b)). We further tested berberine and palmatine for RMS tumorspheres in three-dimensional (3D) culture to evaluate their activities in a condition similar to tumorigenesis.

Materials and methods

Compounds

Berberine hydrochloride (Nacalai, Osaka, Japan) and palmatine chloride hydrate (Nacalai) were dissolved in sterile water. In experiments of berberine or palmatine, an equal volume of sterile water instead of the test sample served as a negative control.

RMS cells

Human RMS cells were provided by JCRB Cell Bank (National Institutes of Biomedical Innovation, Health and Nutrition, Osaka, Japan). ERMS1 cells (JCRB1648) were derived from an anaplastic pelvic ERMS of a 5-year-old female [15]. KYM1 cell strain (JCRB0627) was established from a neck tumor in a 9-month-old infant [16]. RD cells (JCRB9072) were directly derived from the biopsy specimens of a malignant pelvic ERMS of a 7-year-old female patient [17]. All RMS cells were cultured in RPMI1640 (Nacalai) with 10% fetal bovine serum (HyClone; GE Healthcare, UT, USA), 100 units/ml penicillin, and 100 µg/ml streptomycin at 37°C with 5% CO_2.

Cell counting

5.0×10^4 RMS cells/well were seeded on 12-well (ERMS1 and RD) or 24-well (KYM1) plates. On the next day, the cells were treated by replacing the medium with a brand-new medium containing berberine or palmatine. The cells were continuously cultured until their numbers were counted. For cell

109 counting, the cells were completely dissociated by treating with 0.25%
110 trypsin with 1 mM EDTA (Wako, Osaka, Japan) for 5 min at 37°C. The
111 number of cells was counted using a hemocytometer.
112
113 *Cell cycle assay*
114 2.0×10^5 (ERMS1 and RD) or 4.0×10^5 (KYM1) cells/well were seeded on
115 12-well plate. On the next day, the cells were treated by replacing the
116 medium with a brand-new medium containing 10 μM of berberine or
117 palmatine. After 24 h, the cell cycle phases were visualized using Cell-Clock
118 Cell Cycle Assay Kit (Biocolor Life Science Assays, County Antrim, UK). The
119 ratio of the cells at each phase was counted using ImageJ software (National
120 Institute of Health, USA).
121
122 *Fluorescent microscopy*
123 Intracellular incorporation of berberine or palmatine was detected as green
124 fluorescence because berberine and palmatine have fluorescence emissions
125 at 530 nm upon excitations [18,19]. Phase-contrast and fluorescent images
126 were taken and layered using EVOS FL Auto microscope with an emission
127 bandpass filter of 510-542 nm (AMAFD1000; Thermo Fisher Scientific, MA,
128 USA).
129
130 *Quantitative real-time RT-PCR (qPCR)*
131 For 2D culture, 1.5×10^5 (ERMS1 and RD) or 2.0×10^5 (KYM1) cells were
132 seeded on 30-mm dishes. On the next day, the cells were treated by replacing

the medium with a brand-new medium containing 10 μM of berberine or palmatine. After 48 h (KYM1) or 72 h (ERMS1 and RD), the total RNA from the RMS cells was isolated using TRIzol Reagent (Thermo Fisher Scientific) and reverse transcribed using ReverTra Ace qPCR RT Master Mix (TOYOBO, Osaka, Japan). For 3D culture, the RD tumorspheres at day 6 formed as described below were subjected to RNA preparation. qPCR was performed using GoTaq qPCR Master Mix (Promega, WI, USA) with StepOne Real-Time PCR System (Thermo Fisher Scientific). The amount of each transcript was normalized to that of *GAPDH*. The results are presented as fold-change. Primer sequences are described in Table 1.

Western blotting

8.0×10^5 ERMS1 cells were seeded on 100-mm dishes. The cells were treated with 10 μM of berberine or palmatine for 72 h. The whole cell lysate from the cells was harvested using lysis buffer (100 mM Tris-HCl, 75 mM NaCl, and 1% Triton-X100) with protease inhibitors (1 mM 4-(2-aminoethyl)benzenesulfonyl fluoride hydrochloride, 0.8 μM aprotinin, 15 μM E-64, 20 μM leupeptin hemisulfate monohydrate, 50 μM bestatin, and 10 μM pepstatin A) (Nacalai). Then the lysates were denatured with 50 mM Tris-HCl, 10% glycerol, and 2% sodium dodecyl sulfate (SDS) at 95°C for 5 min. 20 μg of protein samples were subjected to SDS-polyacrylamide gel electrophoresis and following Western blotting using iBlot 2 Dry Blotting System (Thermo Fisher Scientific). Rabbit polyclonal anti-$p57^{Kip2}$ (Cell Signaling Technology) (1:1000) and mouse monoclonal anti-GAPDH (5A12;

157 Wako) (1:1000) antibodies were used as primary antibodies. 0.1 ng/ml of
158 horseradish peroxidase (HRP)-conjugated goat anti-rabbit and anti-mouse
159 IgG antibodies (Jackson ImmunoResearch, PA, USA) were used as secondary
160 antibodies, respectively. HRP signal was detected using ECL Prime reagents
161 and ImageQuant LAS 500 (GE Healthcare). The amounts of $p57^{Kip2}$ was
162 normalized to those of GAPDH using ImageJ software.
163
164 *3D culture of RD tumorspheres*
165 The RD cells were dissociated and suspended in 3D Tumorsphere Medium
166 XF (PromoCell, Heidelberg, Germany). 300 cells/30 µl of drops were placed
167 on 24-well floating-culture plates (Sumitomo Bakelite, Tokyo, Japan).
168 Subsequently, the plates were turned over for hanging-drop culture. After 3
169 days, the plates were turned over again, then 300 µl/well of 3D Tumorsphere
170 Medium XF with 10 µM of berberine or palmatine was added to RD
171 tumorspheres (defined as day 0). RD tumorspheres were maintained without
172 medium exchange. Phase-contrast images of the tumorspheres were taken
173 using EVOS FL Auto microscope. The projected areas of the tumorspheres
174 were quantified using ImageJ software.
175
176 *Molecular docking simulation*
177 Molecular models of berberine and palmatine were built by gaussian 09
178 (Gaussian, CT, USA) and antechamber [20]. The force fields except for the
179 partial charges were taken from a general amber force field (GAFF) [21]. The
180 partial charges on the molecules were assigned by a restrained electrostatic

potential (RESP) method based on the conformations after quantum-mechanics structural optimization with B3LYP/6-31G*. These molecular models of berberine and palmatine were used for the following docking simulation. The docking simulation was conducted for berberine or palmatine onto calmodulin. The structures of calmodulin and receptor retinoid X receptor α ligand-binding domain (RXRα-LBD) were taken from the D chain of PDB ID 1K90 and 3OAP, respectively. The amber force field, ff99 [22], was used for the protein model. We used the docking software Sievgene [23]. The docking pose with the lowest docking score was stored. Finally, each complex structure of berberine and palmatine docking upon calmodulin was obtained.

Statistical analysis

The results are presented as the mean ± standard error. Statistical comparisons were performed using multiple comparison test with Williams' test or Scheffe's F test, where appropriate following one-way analysis of variance (ANOVA). Statistical significance was set at a p value < 0.05.

Results

Berberine but not palmatine inhibits the growth of ERMS1 cells

ERMS1 is an ERMS cell line having c.743G>T mutation on *TP53* gene [15]. The ERMS1 cells showed spindle or polygonal shape in the two-dimensional (2D) monolayer culture (Figure 1(b)). First, apoptotic effects of berberine and palmatine on ERMS1 cells were examined. qPCR results indicated that mRNA levels of a apoptosis-inducing gene, Bax (*BAX*), and an anti-apoptotic factor, Bcl-xL (*BCL2L1*), were not altered within 24 h even by 100 μM of berberine or palmatine (Figure 1(c)). Then, the effects of berberine and palmatine at lower concentrations on cell cycle were investigated. The number of ERMS1 cells treated with 1, 3, or 10 μM of berberine was counted every 24 h as an index of cell growth (Figure 2(a)). Berberine suppressed ERMS1 cell growth in a dose-dependent manner. Berberine at concentration of 3 and 10 μM significantly reduced the number of ERMS1 cells at 72 h of treatment. Even 1 μM of berberine suppressed the growth by 96 h. However, 10 μM of palmatine did not show any growth inhibition on ERMS1 cells (Figure 2(b)). Microscopic observation also displayed a berberine-dependent reduction of the ERMS1 cell number. There was no other obvious alteration, such as morphological change or cell death by berberine or palmatine (Figure 2(c)). Cell cycle phases of the live ERMS1 cells treated by 10 μM of berberine or palmatine were monitored using the redox dye which stains mitotic cells at M phase in dark blue, pre-mitotic cells at S/G_2 phase in green, and non-mitotic cells G_1 phase in pale yellow. After 24 h of treatment, berberine

223 but not palmatine dramatically increased the cells at G_1 phase and inhibited
224 to enter into S/G_2 phase (Figure 2(d)). It clearly indicated that berberine
225 induces G_1 cell cycle arrest in ERMS1 cells. The uptake of berberine or
226 palmatine into ERMS1 cells was detected by the green fluorescence
227 generated by berberine or palmatine (Figure 2(e)). Berberine was
228 incorporated into the ERMS1 cells within 24 h. Palmatine incorporation was
229 similarly detected, but the intensity of the fluorescence was lower than that
230 of berberine. It may be one of the reasons why the growth inhibitory effect of
231 palmatine was relatively weaker than that of berberine.
232
233 ***Berberine but not palmatine inhibits the growth of KYM1 cells***
234 The KYM1 cells displayed small lymphocyte-like round shape with mild
235 adhesion to the culture plates in 2D culture (Figure 1(b)). Treatment of 100
236 μM of berberine or palmatine for 24 h did not alter the expression levels of
237 *BAX* and *BCL2L1* in KYM1 cells (Figure 1(c)). However, berberine
238 suppressed the growth of KYM1 cells in a dose-dependent manner (Figure
239 3(a)). KYM1 cells were more sensitive to berberine as compared to the
240 ERMS1 cells. The number of KYM1 cells was significantly reduced 48 h after
241 berberine treatment for every dose. In particular, 10 μM of berberine
242 completely arrested KYM1 cell growth. However, 10 μM of palmatine did not
243 inhibit the expansion of KYM1 cells (Figure 3(b)). In microscopic observation,
244 the confluent KYM1 cells were attached to the culture plates tightly, but the
245 berberine-treated KYM1 cells maintained the globular morphology probably
246 because of the low-density of the cells (Figure 3(c)). Cell cycle assays clearly

showed that KYM1 cells were significantly arrested at G_1 phase by berberine but not by palmatine (Figire 3(d)). Berberine was incorporated into the KYM1 cells within 24 h, whereas palmatine was scarcely detected inside the cells (Figure 3(e)).

Berberine and palmatine inhibit the growth of RD cells

RD is a malignant ERMS cell strain having amplification of the *MYC* gene, p.Gln61His mutation on the *NRAS* gene, and c.248C>T homozygous mutation on the *TP53* gene [24-26] (Figure 1(b)). Although berberine and palmatine did not affect apoptotic gene expression (Figure 1(c)), berberine inhibited the outgrowth of RD cells in a dose-dependent manner (Figure 4(a)). The sensitivity of the RD cells to berberine was moderate; it significantly reduced the number of RD cells at 72 h after treatment in every dose. Intriguingly, 10 μM of palmatine markedly suppressed the RD cell growth (Figure 4(b)). Although the inhibitory effect of palmatine was milder than that of berberine at the same dose, a reduced number of palmatine-treated cells was also observed by microscopy (Figure 4(c)). In the berberine-treated RD cells, atrophic morphology was observed in addition to growth inhibition. 10 μM of berberine but not of palmatine rapidly induced G_1 cell cycle arrest in RD cells within 24 h (Figure 4(d)). Green fluorescent images indicated that both berberine and palmatine were incorporated into the RD cells within 24 h (Figure 4(e)). As observed in the ERMS1 and KYM1 cells, the uptake of palmatine into the RD cells was fewer than that of berberine.

These differences between berberine and palmatine at early stage of the treatment would be involved in their disparities of growth inhibitory effects.

Berberine modulates cyclin-related gene expression in the RMS cells

qPCR quantified the expression of proliferation marker Ki-67 (*MKI67*) and G_1 phase-involved genes, cyclin D1 (*CCND1*) and cyclin-dependent kinase inhibitor 1C ($p57^{Kip2}$) (*CDKN1C*), in the berberine- or palmatine-treated RMS cells (Figure 5(a)). As well as the results of cell cycle assays, *MKI67* levels were significantly decreased by berberine in KYM1 and RD cells. Berberine did not alter *CCND1* levels in any RMS cells. While, by berberine treatment, *CDKN1C* levels were significantly upregulated in ERMS1 cells and tended to be induced in RD cells. Accordingly, protein level of $p57^{Kip2}$ was markedly increased in the berberine-treated ERMS1 cells (Figure 5(b)). On the other hand, expression levels of *MKI67*, *CCND1*, and *CDKN1C* were not altered at all by palmatine in any RMS cells. Both berberine and palmatine did not affect mRNA levels of *BAX* and *BCL2L1*. These data demonstrate that berberine inhibits RMS cell growth, in part, by modulating cell cycle-related gene expression.

Berberine and palmatine inhibit the growth of 3D-cultured RD tumorspheres

To examine the effects of berberine analogs on the growth of tumorspheres in a xeno-free condition, we tried to establish a novel 3D culture method for RMS cells. To form initial aggregation, the drops containing 300 RD cells

were subjected to hanging-drop culture for 3 days. The spheres formed in the drops (defined as day 0) were subsequently maintained in floating culture. These RD tumorspheres continued to grow at least for 12 days without medium exchange, and finally their diameters reached 0.5-1.0 mm (Figure 6(a)). Although both berberine and palmatine were uptaken into RD tumorspheres within 24 h (Figure 6(b)), incorporation of palmatine was fewer than that of berberine as observed in 2D culture (Figure 4(e)). It demonstrates that this 3D culture system is applicable to investigate the effects of anti-tumor drugs. The growth ratio of the RD tumorspheres treated with 10 μM of berberine or palmatine was quantified as to their projected areas (Figure 6(c,d)). Both berberine and palmatine completely inhibited the growth of the spheres for 10 days without medium exchange. The projected areas were not different between berberine- and palmatine-treated tumorspheres. It is not corresponded to the results of 2D culture indicating that the inhibitory effect of palmatine was weaker than that of berberine (Figure 4(b)). As shown in Figure 6(e), *MKI67* expression in RD tumorspheres was significantly reduced by berberine but not by palmatine. Confusingly, palmatine treatment decreased the mRNA level of *CDKN1C*. Expression levels of *BAX* and *BCL2L1* were not altered by berberine nor palmatine. These data suggests that palmatine did not arrest cell cycle and not induce apoptosis in 3D-cultured RD tumorsphere as well in 2D-cultured RD cells. These results demonstrate that berberine and palmatine were able to serve as growth inhibitors for RMS tumors but their mechanism of actions will be different.

Discussion

This is the first study to report that berberine inhibits the growth of multiple ERMS cell lines; ERMS1, KYM1, and RD. Palmatine also suppressed the expansion of RD cells but not that of ERMS1 and KYM1 cells. Distinct effects between berberine and palmatine suggest that it is possible to develop more effective anti-tumor molecules through modifications of berberine. It has been reported that protoberberine-type alkaloids, such as palmatine, coptisine, and jatrorrhizine, exhibit similar bioactivities to berberine [1]. Previous studies have reported the growth inhibitory effect of palmatine on prostate cancer [27], that of coptisine on lung cancer [28], and that of jatrorrhizine on melanoma cells [29]. However, these actions of berberine analogs have not been directly compared. Precise differences of the anti-tumor effects among the berberine derivatives should be evaluated in further studies which will contribute to identifying the most effective molecule for each tumor.

Berberine analogs are water-soluble and cell-permeable small alkaloids (molecular weights; ~350). According to the results of absorption, distribution, metabolism, and excretion (ADME) parameter prediction [30], there is not much difference between the consensus values of *n*-octanol/water partition coefficient (Consensus Log $P_{o/w}$) of berberine (2.55) and palmatine (2.64). It suggests that berberine and palmatine have the same cell membrane permeability. However, this study showed that intracellular incorporation of palmatine was lower than that of berberine in every RMS

cell line. Correspondingly, it has been reported that intracellular concentrations of palmatine is around one-sixth compared to that of berberine in the colon cancer Caco2 cells treated with 10 μM of berberine or palmatine for 1 h. Their intracellular amounts were significantly increased by the inhibitors of P-glycoprotein (P-gp) which is a member of ATP-binding cassette (ABC) transporter family [31]. These data demonstrates that berberine analogs are P-gp substrates, and their different affinities to P-gp may affect ABC transporter-mediated uptake.

Cell cycle assays and *MKI67* expression analyses clearly indicated that berberine treatment induces cell cycle arrest at G_1 phase in every RMS cell line as observed in the other types of cells [32]. Previous studies reported that berberine suppresses *CCND1* in cholangiocarcinoma [33] and hepatoma [34], or induces *CDKN1C* in human mesenchymal stem cells [35]. Berberine did not decrease *CCND1* mRNA in any RMS cells but actually upregulated *CDKN1C* mRNA and $p57^{Kip2}$ protein in ERMS1 cells. These results demonstrate that berberine inhibits RMS cell growth, in part, by inducing G_1 cell cycle arrest.

Some molecules have been reported as the direct intracellular targets of berberine. A previous study performed computational screening and identified calmodulin, a Ca^{2+}-binding protein, as a putative target of berberine [7]. It has been reported that inhibition of calmodulin induces G_1 cell cycle arrest in cancer cells [36]. Indeed, berberine-induced G_1 arrest in hepatoma cells was enhanced by cotreatment of calmodulin inhibitors [7]. Our docking simulation also illustrated that berberine can fit into the pocket

of the calmodulin structure (Figure 7(a)). Similarly, palmatine fits within the same pocket of calmodulin with a binding score equal to that of berberine ($\Delta G = -6.7$ kcal/mol) (Figure 7(b)). However, the interactive positions relative to calmodulin are different between berberine and palmatine.

Other study reported that berberine directly targets nuclear RXRα to promote interaction with ß-catenin, which finally leads cell cycle arrest of colon cancer cells [37]. Our docking simulation predicted that both berberine and palmatine can bind to RXRα-LBD with high affinities; the binding scores of berberine and palmatine are −9.6 and −8.0 kcal/mol, respectively. However, their binding poses on RXRα-LBD are different (Figure 7(c,d)). Their structural properties of binding poses affect the conformation of RXRα, which may be involved in RXRα activation toward ß-catenin degradation.

These findings provide the viewpoint that structural and binding differences of berberine derivatives on their target proteins are closely related to their incorporations and anti-tumor effects. Thus, screening of natural or synthesized berberine derivatives will be a powerful strategy to develop novel RMS inhibitors for tailored chemotherapy. For this purpose, we tried to establish a xeno-free 3D culture method for RMS cells to evaluate the growth inhibitory effects of the drugs. Two recent studies have described the 3D culture systems for RMS cells based on cell sheet or collagen disk technology [38,39]. However, it has not been reported the formation of RMS tumorspheres in floating culture. It is generally considered that sphere culture selectively exploits inherent characters of stem cells including cancer stem cells [40]. The present study successfully generated tumorspheres of

391 RD cells by a hanging drop-based floating culture, which is a convenient and
392 reproducible system to continuously evaluate the growth of RMS cells and
393 the effects of their inhibitors in 3D condition for more than ten days. Using
394 this system, we confirmed that both berberine and palmatine intensively
395 inhibited the expansion of RD tumorspheres. It proves that our 3D culture is
396 conceptually valid for drug screening. Incorporation of palmatine into RD
397 tumorspheres was relatively lower than that of berberine as into the
398 2D-cultured RD cells. Although palmatine did not arrest cell cycle or not
399 induce apoptosis, palmatine completely inhibited the growth of RD
400 tumorspheres as berberine did. A recent study reported that palmatine
401 inhibits reciprocal interaction between pancreatic stellate cells and cancer
402 cells through suppressing activation of type 1 collagen, which is one of the
403 components of tumor microenvironment [41]. Dense intercellular interaction
404 within the tumor microenvironment is essential for tumor cell survival and
405 growth. As in pancreatic cells, palmatine might decrease collagen
406 accumulation, interfere extracellular matrix formation, and finally inhibit
407 growth of RD tumorspheres. It will be a possible mechanism that palmatine
408 showed graded growth inhibitory effects among RMS cell lines or between
409 2D and 3D culture systems.

410 Growing evidences have been showing that the 2D-cultured cells
411 deviate from physiological responses under some circumstances by its own
412 cell bioactivities. 3D culture systems are considered to be better to mimic *in*
413 *vivo* condition [40]. In our study, sensitivities of palmatine to RD cells were
414 actually differ between 2D and 3D culture systems. Establishing robust 3D

415 culture methods for screening will contribute to explore the molecules which
416 have appropriate drug efficacies *in vivo*. Unfortunately, tumorspheres of
417 ERMS1 and KYM1 cells have not been formed yet. The culture system
418 should be optimized and improved to apply the method to various sarcoma
419 cells. Reconstruction of the tumor microenvironment will be essentially
420 important to recapitulate the actions of anti-tumor molecules, such as
421 berberine analogs *in vitro*.
422

Author contributions

TT designed the study. TT and KU wrote the manuscript. SS, SN, and YN performed the experiments. KU performed the docking simulation. All authors have read and approved the final manuscript.

Acknowledgments

This study was supported in part by Grants-in-Aid from The Japan Society for the Promotion of Science (16K19397) and from The Morinaga Foundation for Health and Nutrition to TT, and a Grant-in-Aid from The Fund of Nagano Prefecture to Promote Scientific Activity (H30-3-3) to SS.

Disclosure statement

No potential conflict of interests was reported by the authors.

References

[1] Meng FC, Wu ZF, Yin ZQ, et al. Coptidis rhizoma and its main bioactive components: recent advances in chemical investigation, quality evaluation and pharmacological activity. Chin Med. 2018; 13: 13.

[2] Cheng YT, Yang CC, Shyur LF. Phytomedicine-modulating oxidative stress and the tumor microenvironment for cancer therapy. Pharmacol Res. 2016; 114: 128-143.

[3] Mantena SK, Sharma SD, Katiyar SK. Berberine, a natural product, induces G1-phase cell cycle arrest and caspase-3-dependent apoptosis in human prostate carcinoma cells. Mol Cancer Ther. 2006; 5: 296-308.

[4] Yan K, Zhang C, Feng J, et al. Induction of G1 cell cycle arrest and apoptosis by berberine in bladder cancer cells. Eur J Pharmacol. 2011; 661: 1-7.

[5] James MA, Fu H, Liu Y, et al. Dietary administration of berberine or Phellodendron amurense extract inhibits cell cycle progression and lung tumorigenesis. Mol Carcinog. 2011; 50: 1-7.

[6] Chidambara Murthy KN, Jayaprakasha GK, Patil BS. The natural alkaloid berberine targets multiple pathways to induce cell death in cultured human colon cancer cells. Eur J Pharmacol. 2012; 688: 14-21.

[7] Ma C, Tang K, Liu Q, et al. Calmodulin as a potential target by which berberine induces cell cycle arrest in human hepatoma Bel7402 cells. Chem Biol Drug Des. 2013; 81: 775-783.

[8] Liu Z, Liu Q, Xu B, et al. Berberine induces p53-dependent cell cycle arrest and apoptosis of human osteosarcoma cells by inflicting DNA damage. Mutat Res. 2009; 662: 75-83.

[9] Eo SH, Kim JH, Kim SJ. Induction of G_2/M arrest by berberine via activation of PI3K/Akt and p38 in human chondrosarcoma cell line. Oncol Res. 2014; 22: 147-157.

[10] Sun X, Guo W, Shen JK, et al. Rhabdomyosarcoma: Advances in molecular and cellular biology. Sarcoma. 2015; 2015: 232010.

[11] Kikuchi K, Tsuchiya K, Otabe O, et al. Effects of PAX3-FKHR on malignant phenotypes in alveolar rhabdomyosarcoma. Biochem Biophys Res Commun. 2008; 365: 568-574.

[12] Jothi M, Nishijo K, Keller C, et al. AKT and PAX3-FKHR cooperation enforces myogenic differentiation blockade in alveolar rhabdomyosarcoma cell. Cell Cycle. 2012; 11: 895-908.

[13] Rubin BP, Nishijo K, Chen HI, et al. Evidence for an unanticipated relationship between undifferentiated pleomorphic sarcoma and embryonal rhabdomyosarcoma. Cancer Cell. 2011; 16: 177-191.

[14] Yang L, Takimoto T, Fujimoto J. Prognostic model for predicting overall survival in children and adolescents with rhabdomyosarcoma. BMC Cancer. 2014; 14: 654.

[15] Nishimura R, Takita J, Sato-Otsubo A, et al. Characterization of genetic lesions in rhabdomyosarcoma using a high-density single nucleotide polymorphism array. Cancer Sci. 2013; 104: 856-864.

[16] Sekiguchi M, Shiroko Y, Suzuki T, et al. Characterization of a human rhabdomyosarcoma cell strain in tissue culture. Biomed Phamacother. 1985; 39: 372-380.

[17] McAllister RM, Melnyk J, Finkelstein JZ, et al. Cultivation in vitro of cells derived from a human rhabdomyosarcoma. Cancer. 1969; 24: 520-526.

[18] Guo Y, Chen Y, Wei Y, et al. Label-free fluorescent aptasensor for potassium ion using structure-switching aptamers and berberine. Spectrochim Acta A Mol Biomol Spectrosc. 2015; 136: 1635-1641.

[19] Mi R, Tu B, Bai XT, et al. Binding properties of palmatine to DNA: spectroscopic and molecular modeling investigations. Luminescence. 2015; 30: 1344-1351.

[20] Wang J, Wang W, Kollman PA, et al. Automatic atom type and bond type perception in molecular mechanical calculations. J Mol Graph Model. 2006; 25: 247-260.

[21] Wang J, Wolf RM, Caldwell JW, et al. Development and testing of a general amber force field. J Comput Chem. 2004; 25: 1157-1174.

[22] Wang J, Cieplak P, Kollman PA. How well does a restrained electrostatic potential (RESP) model perform in calculating conformational energies of organic and biological molecules? J Comput Chem. 2000; 21: 1049-1074.

[23] Fukunishi F, Mikami Y, Nakamura H. Similarities among receptor pockets and among compounds: Analysis and application to in silico ligand screening. J Mol Graph Model. 2005; 24: 34-45.

[24] Hinson ARP, Jones R, Crose LES, et al. Human rhabdomyosarcoma cell lines for rhabdomyosarcoma research: utility and pitfalls. Front Oncol. 2013; 3: 183.

[25] Felix CA, Kappel CC, Mitsudomi T, et al. Frequency and diversity of p53 mutations in childhood rhabdomyosarcoma. Cancer Res. 1992; 52: 2243-2247.

[26] Miyachi M, Kakazu N, Yagyu S, et al. Restoration of p53 pathway by nutlin-3 induces cell cycle arrest and apoptosis in human rhabdomyosarcoma cells. Clin Cancer Res. 2009; 15: 4077-4084.

[27] Hambright HG, Batth IS, Xie J, et al. Palmatine inhibits growth and invasion in prostate cancer cell: Potential role for rpS6/NFκB/FLIP. Mol Carcinog. 2015; 54: 1227-1234.

[28] Rao PC, Begum S, Sahai M, et al. Coptisine-induced cell cycle arrest at G2/M phase and reactive oxygen species-dependent mitochondria-mediated apoptosis in non-small-cell lung cancer A549 cells. Tumor Biol. 2017; 39: 1010428317694565.

[29] Liu R, Cao Z, Pan Y, et al. Jatrorrhizine hydrochloride inhibits the proliferation and neovascularization of C8161 metastatic melanoma cells. Anticancer Drugs. 2013; 24: 667-676.

[30] Daina A, Michielin O, Zoete O. SwissADME: a free web tool to evaluate pharmacokinetics, drug-likeness and medicinal chemistry friendliness of small molecules. Sci Rep. 2017; 7: 42717.

[31] Zhang X, Qiu F, Jiang J, et al. Intestinal absorption mechanisms of berberine, palmatine, jateorhizine, and coptisine: involvement of P-glycoprotein. Xenobiotica. 2011; 41: 290-296.

[32] Bailon-Moscoso N, Cevallos-Solorzano G, Romero-Benavides JC, et al. Natural compounds as modulators of cell cycle arrest: application for anticancer chemotherapies. Curr Genomics. 2017; 18: 106-131.

[33] He W, Wang B, Zhuang Y, et al. Berberine inhibits growth and induces G1 arrest and apoptosis in human cholangiocarcinoma QBC939 cells. J Pharmacol Sci. 2012; 119: 341-348.

[34] Wang N, Wang X, Tan HY, et al. Berberine suppresses cyclin D1 expression through proteasomal degradation in human hepatoma cells. Int J Mol Sci. 2016; 17: E1899.

[35] Ke T, Deming X, Jian W, et al. Berberine promotes bone marrow-derived mesenchymal stem cells osteogenic differentiation via canonical Wnt/ß-catenin signaling pathway. Toxicol Lett. 2016; 240: 68-80.

[36] Shim JS, Lee J, Kim KN, et al. Development of a new Ca^{2+}/calmodulin antagonist and its anti-proliferative activity against cololectal cancer cells. Biochem Biophys Res Commun. 2007; 359: 747-751.

[37] Ruan H, Zhan YY, Hou J, et al. Berberine binds RXRα to suppress ß-catenin signaling in colon cancer cells. Oncogene. 2017; 36: 6906-6918.

[38] Li M, Nagamori E, Kino-oka M. Disruption of myoblast alignment by highly motile rhabdomyosarcoma cell in tissue structure. J Biosci Bioeng. 2017; 123: 259-264.

552 [39] Moghadam AR, da Silva Rosa SC, Samiei E, et al. Autophagy modulates
553 temozolomide-induced cell death in alveolar rhabdomyosarcoma cells.
554 Cell Death Discov. 2018; 4: 52.
555 [40] He J, Xiong, L, Li Q, et al. 3D modeling of cancer stem cell niche.
556 Oncotarget. 2018; 9: 1326-1345.
557 [41] Chakravarthy D, Munoz AR, Su A, et al. Palmatine suppresses
558 glutamine-mediated interaction between pancreatic cancer and stellate
559 cells through simultaneous inhibition of survivin and COL1A1. Cancer
560 Lett. 2018; 419: 103-115.
561 [42] Lu J, Zhang Q, Tan D, et al. GABA A receptor π subunit promotes
562 apoptosis of HTR-8/SVneo trophoblastic cells: Implications in
563 preeclampsia. Int J Mol Med. 2016; 38: 105-112.
564 [43] Yosef R, Pilpel N, Tokarsky-Amiel R, et al. Directed elimination of
565 senescent cells by inhibition of BCL-W and BCL-XL. Nat Commun. 2016;
566 7: 11190.
567 [44] Kumari S, Puneet, Prasad SB, et al. Cyclin D1 and cyclin E2 are
568 differentially expressed in gastric cancer. Med Oncol. 2016; 33: 40.
569 [45] Ueberberg S, Tannapfel A, Schenker P, et al. Differential expression of
570 cell-cycle regulators in human beta-cells derived from insulinoma tissue.
571 Metabolism. 2016; 65: 736-746.
572 [46] Sharma V, Harafuji N, Belayew A, et al. DUX4 differentially regulates
573 transcriptomes of human rhabdomyosarcoma and mouse C2C12 cells.
574 PLoS One. 2013; 8: e64691.
575

576 **Table 1. Primer sequences for qPCR.**

Gene	Sequence (5'- 3')	Reference
BAX	GCTGGACATTGGACTTCCTC CTCAGCCCATCTTCTTCCAG	[42]
BCL2L1	GGCCACTTACCTGAATGACC AAGAGTGAGCCCAGCAGAAC	[43]
CCND1	CCTCGGTGTCCTACTTCAAA GGGATGGTCTCCTTCATCTT	[44]
CDKN1C	GGCCTCTGATCTCCGATTTCTTC GGGTCTGCTCCACCGAG	[45]
GAPDH	TGTCAAGCTCATTTCCTGGTA GTGAGGGTCTCTCTCTTCCTCTTGT	[46]
MKI67	AAGAGGTGTGCAGAAAATCCAAAG CTTCACTGTCCCTATGACTTCTGGTT	[45]

577

Figure legends

Figure 1. Berberine derivatives and human RMS cells.

(a) The structural formula of berberine derivatives. (b) 2D-cultured human RMS cells. Scale bar, 100 μm. (c) qPCR results of gene expression in RMS cells treated with 10 or 100 μM of berberine or palmatine for 24 h. The mean value in control RMS cells was set at 1.0 for each gene. There was no significant difference among samples in any RMS cells (Scheffe's F test). n = 3.

Figure 2. Effects of berberine and palmatine on ERMS1 cell growth.

(a) The number of ERMS1 cells treated with 1, 3, or 10 μM of berberine. * p < 0.05, ** p < 0.01 vs 0 μM at each time point (Williams' test). n = 3. (b) The number of ERMS1 cells treated with 10 μM of berberine or palmatine. ** p < 0.01 vs control at each time point (Scheffe's F test). n = 5. (c) Representative images of ERMS1 cells treated with 10 μM of berberine or palmatine for 96 h. Scale bar, 250 μm. (d) Representative images and the ratio of cell cycle phases of ERMS1 cells treated with 10 μM of berberine or palmatine for 24 h. Scale bar, 100 μm. ** p < 0.01 vs control, †† p < 0.01 vs berberine (Scheffe's F test). n = 4. (e) Incorporation of berberine or palmatine into ERMS1 cells as 530 nm emission at 24 h after treatment at a concentration of 10 μM. Scale bar, 100 μm.

Figure 3. Effects of berberine and palmatine on KYM1 cell growth.

602 (a) The number of KYM1 cells treated with 1, 3, or 10 μM of berberine. * $p <$
603 0.05, ** $p < 0.01$ vs 0 μM at each time point (Williams' test). $n = 4$. (b) The
604 number of KYM1 cells treated with 10 μM of berberine or palmatine. ** $p <$
605 0.01 vs control at each time point (Scheffe's F test). $n = 4$. (c) Representative
606 images of KYM1 cells treated with 10 μM of berberine or palmatine for 72 h.
607 Scale bar, 250 μm. (d) Representative images and the ratio of cell cycle
608 phases of KYM1 cells treated with 10 μM of berberine or palmatine for 24 h.
609 Scale bar, 100 μm. ** $p < 0.01$ vs control, †† $p < 0.01$ vs berberine (Scheffe's F
610 test). $n = 4$. (e) Incorporation of berberine or palmatine into KYM1 cells as
611 530 nm emission at 24 h after treatment at a concentration of 10 μM. Scale
612 bar, 100 μm.
613
614 **Figure 4. Effects of berberine and palmatine on RD cell growth.**
615 (a) The number of RD cells treated with 1, 3, or 10 μM of berberine. ** $p <$
616 0.01 vs 0 μM at each time point (Williams' test). $n = 3$. (b) The number of RD
617 cells treated with 10 μM of berberine or palmatine. * $p < 0.05$ vs control, ** p
618 < 0.01 vs control, †† $p < 0.01$ vs berberine at each time point (Scheffe's F test).
619 $n = 4$. (c) Representative images of RD cells treated with 10 μM of berberine
620 or palmatine for 96 h. Scale bar, 250 μm. (d) Representative images and the
621 ratio of cell cycle phases of RD cells treated with 10 μM of berberine or
622 palmatine for 24 h. Scale bar, 100 μm. ** $p < 0.01$ vs control, †† $p < 0.01$ vs
623 berberine (Scheffe's F test). $n = 4$. (e) Incorporation of berberine or palmatine
624 into RD cells as 530 nm emission at 24 h after treatment at a concentration
625 of 10 μM. Scale bar, 100 μm.

626

627 **Figure 5. Berberine inhibits cell cycle gene expression in RMS cells.**

628 (a) qPCR results of gene expression in RMS cells treated with 10 μM of
629 berberine or palmatine for 48 h (KYM1) or 72 h (ERMS1 and RD). The mean
630 value in control RMS cells was set at 1.0 for each gene. * $p < 0.05$ vs control,
631 ** $p < 0.01$ vs control, †† $p < 0.01$ vs berberine (Scheffe's F test). $n = 3$-5. (b)
632 Representative images of Western blotting and the quantified $p57^{Kip2}$ protein
633 levels in the ERMS1 cells treated with 10 μM of berberine or palmatine for
634 72 h. * $p < 0.05$ vs control (Scheffe's F test). $n = 3$.

635

636 **Figure 6. Effects of berberine and palmatine on RD tumorspheres.**

637 (a) The growth of 3D-cultured RD tumorsphere. Scale bar, 200 μm. (b)
638 Incorporation of berberine or palmatine into RD tumorspheres as 530 nm
639 emission at 24 h after treatment at a concentration of 10 μM. Scale bar, 50
640 μm. (c) Projected areas of the RD tumorspheres treated with 10 μM of
641 berberine or palmatine. The mean value of the control tumorspheres on day
642 0 was set at 1.0. ** $p < 0.01$ vs control (Scheffe's F test). $n = 4$-8. (d)
643 Representative images of the RD tumorspheres treated with 10 μM of
644 berberine or palmatine for 8 days. Scale bar, 100 μm. (e) qPCR results of
645 gene expression in RD tumorspheres treated with 10 μM of berberine or
646 palmatine for 6 days. ** $p < 0.01$ vs control, †† $p < 0.01$ vs berberine (Scheffe's
647 F test). $n = 3$.

648

Figure 7. The simulated binding poses of berberine and palmatine on their target proteins.

(a,b) Molecular interactions between calmodulin and berberine analogs. The structures of calmodulin, berberine, and palmatine are colored in gray, yellow, and orange, respectively. (a) The methylenedioxybenzene moiety of berberine is buried in the pocket of calmodulin. (b) The dimethoxybenzene moiety of palmatine interacts with the same pocket as that of berberine. The isoquinoline moiety of palmatine is flipped relative to that of berberine in their bound forms. (c,d) Molecular interactions between RXRα-LBD and berberine analogs. The structures of RXRα-LBD, berberine, and palmatine are colored in gray, yellow, and orange, respectively. (c) Berberine binds to a pocket of RXRα in the vicinity of the other binding pocket for the genuine RXRα ligand. (d) Palmatine attaches to the same pocket that berberine does. The binding pose of palmatine is different from that of berberine.

Figure 1

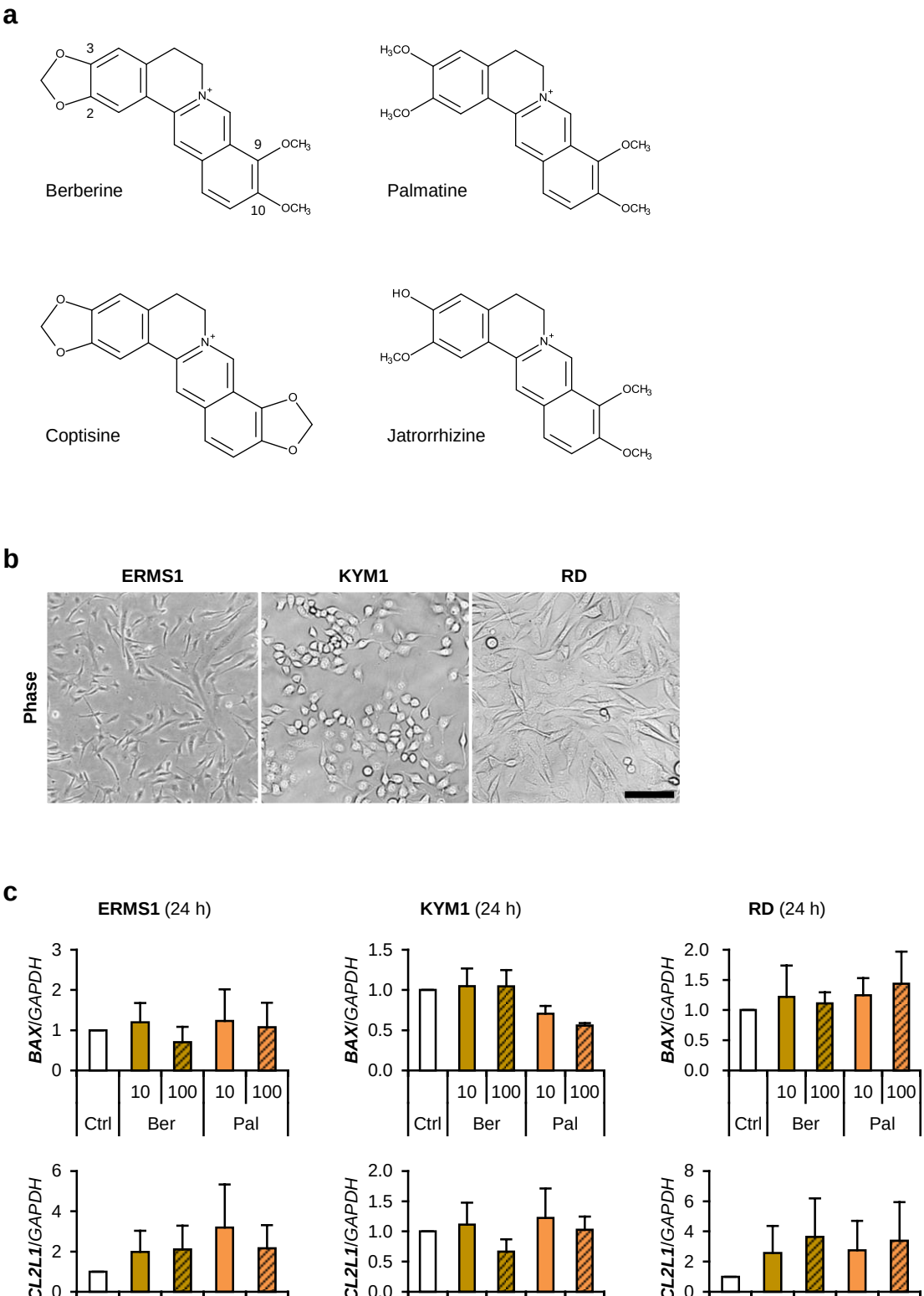
a
Berberine
Palmatine
Coptisine
Jatrorrhizine
b
ERMS1
KYM1
RD
Phase
c
ERMS1 (24 h)
KYM1 (24 h)
RD (24 h)
BAX/GAPDH
BCL2L1/GAPDH
Ctrl
Ber
Pal
10
100

Figure 2

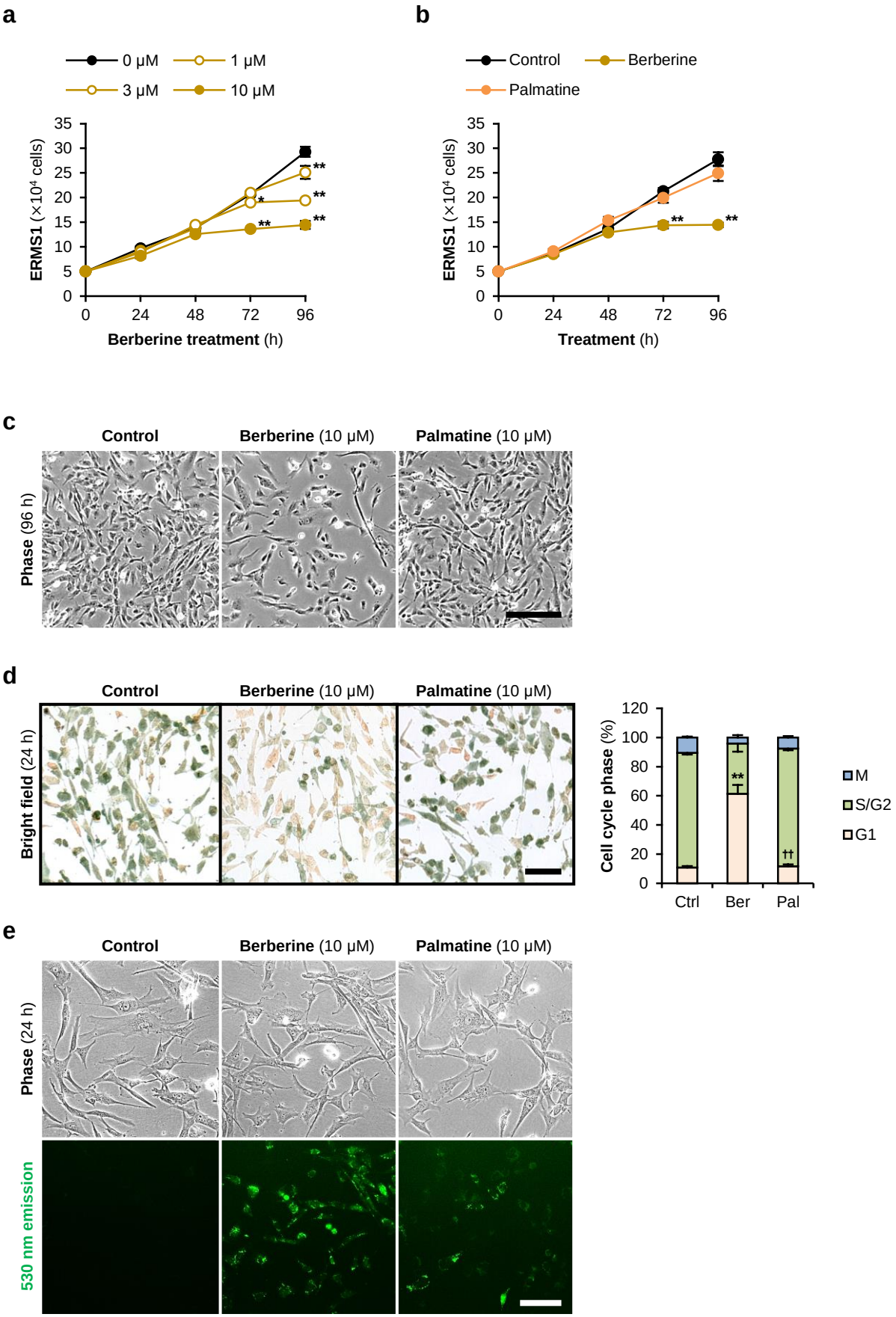
a
0 μM
1 μM
3 μM
10 μM
ERMS1 (×10^4 cells)
Berberine treatment (h)
b
Control
Berberine
Palmatine
ERMS1 (×10^4 cells)
Treatment (h)
c
Control
Berberine (10 μM)
Palmatine (10 μM)
Phase (96 h)
d
Control
Berberine (10 μM)
Palmatine (10 μM)
Bright field (24 h)
Cell cycle phase (%)
Ctrl
Ber
Pal
M
S/G2
G1
e
Control
Berberine (10 μM)
Palmatine (10 μM)
Phase (24 h)
530 nm emission

Figure 3

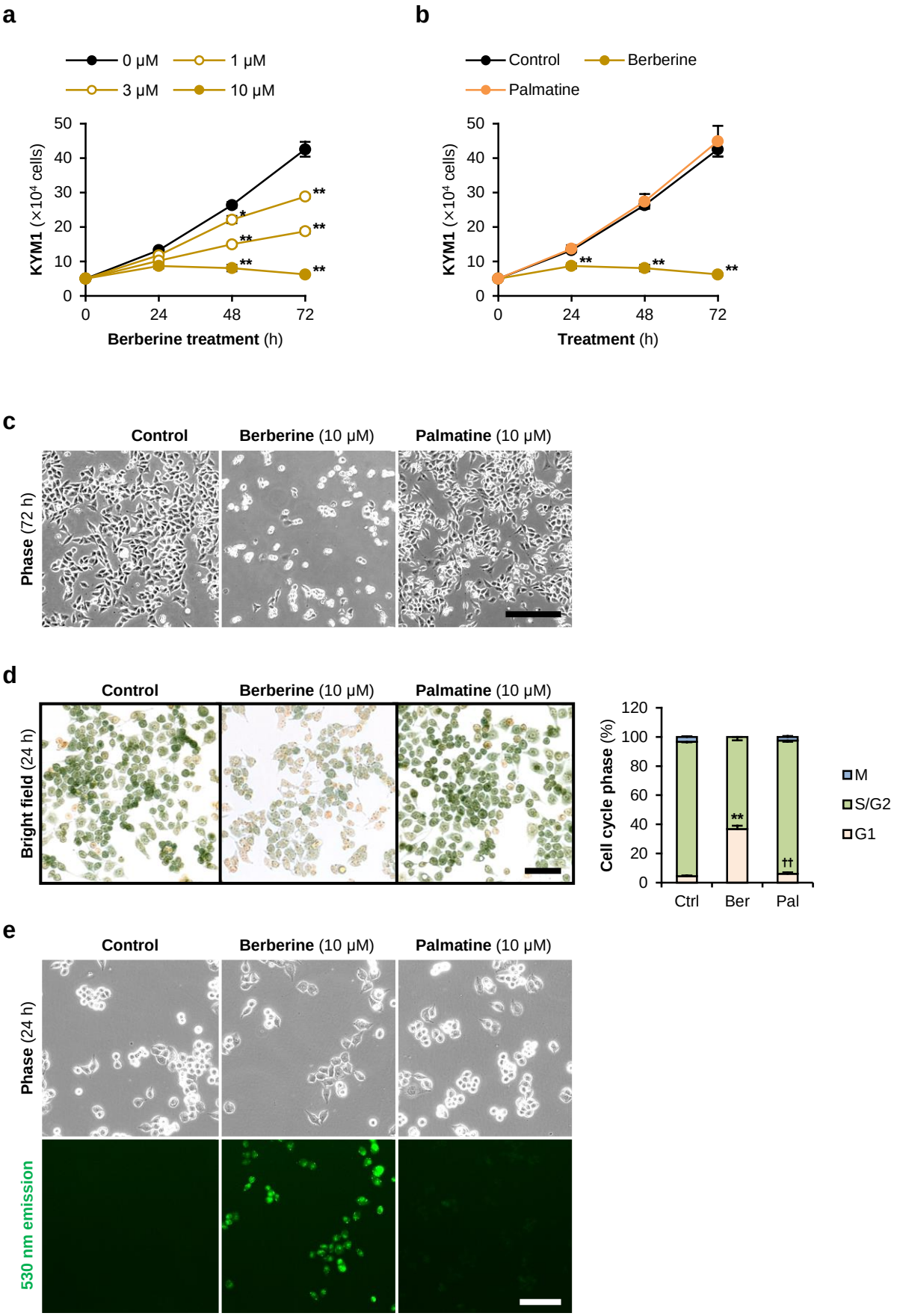
a
0 μM
1 μM
3 μM
10 μM
KYM1 (×10⁴ cells)
Berberine treatment (h)
b
Control
Berberine
Palmatine
KYM1 (×10⁴ cells)
Treatment (h)
c
Control
Berberine (10 μM)
Palmatine (10 μM)
Phase (72 h)
d
Control
Berberine (10 μM)
Palmatine (10 μM)
Bright field (24 h)
Cell cycle phase (%)
Ctrl
Ber
Pal
M
S/G2
G1
e
Control
Berberine (10 μM)
Palmatine (10 μM)
Phase (24 h)
530 nm emission

Figure 4

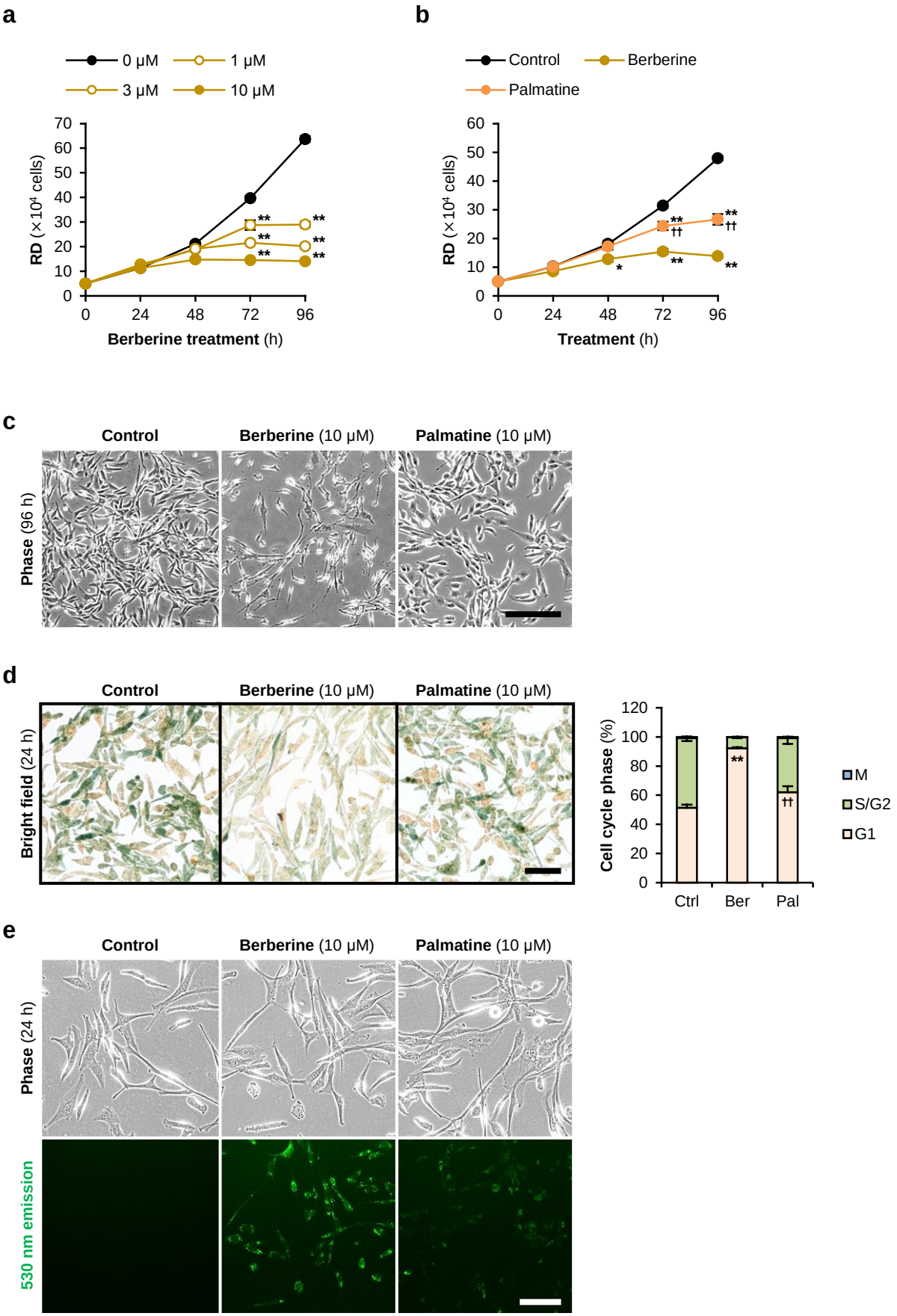
a
0 μM
1 μM
3 μM
10 μM
RD (×10⁴ cells)
Berberine treatment (h)
b
Control
Berberine
Palmatine
RD (×10⁴ cells)
Treatment (h)
c
Control
Berberine (10 μM)
Palmatine (10 μM)
Phase (96 h)
d
Control
Berberine (10 μM)
Palmatine (10 μM)
Bright field (24 h)
Cell cycle phase (%)
Ctrl
Ber
Pal
M
S/G2
G1
e
Control
Berberine (10 μM)
Palmatine (10 μM)
Phase (24 h)
530 nm emission

Figure 5

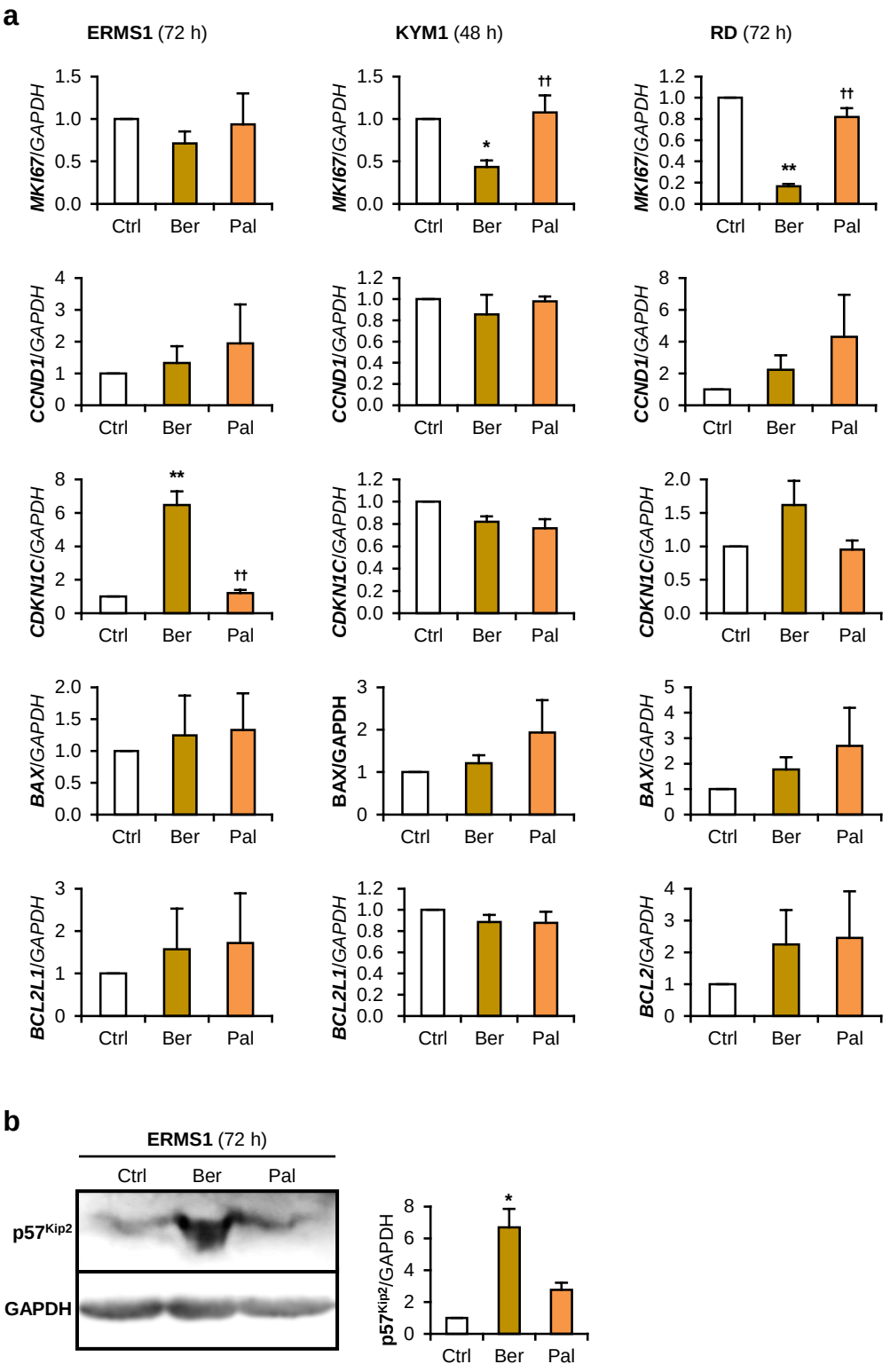
a
ERMS1 (72 h)
KYM1 (48 h)
RD (72 h)
MKI67/GAPDH
CCND1/GAPDH
CDKN1C/GAPDH
BAX/GAPDH
BCL2L1/GAPDH
BCL2/GAPDH
Ctrl
Ber
Pal
b
ERMS1 (72 h)
p57Kip2
GAPDH
p57Kip2/GAPDH

Figure 6

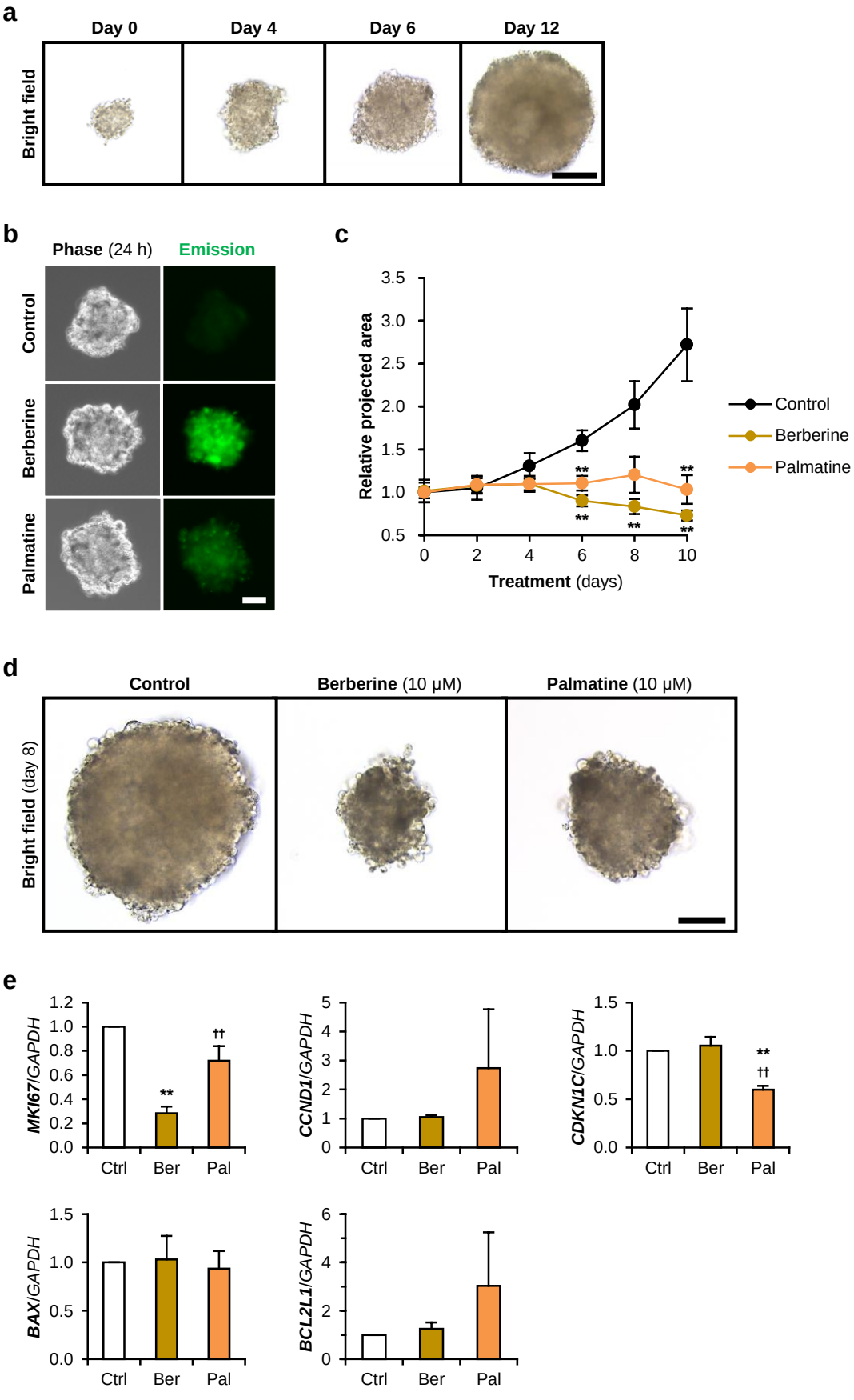
a
Day 0
Day 4
Day 6
Day 12
Bright field
b
Phase (24 h)
Emission
Control
Berberine
Palmatine
c
Relative projected area
Treatment (days)
Control
Berberine
Palmatine
d
Control
Berberine (10 μM)
Palmatine (10 μM)
Bright field (day 8)
e
MKI67/GAPDH
CCND1/GAPDH
CDKN1C/GAPDH
BAX/GAPDH
BCL2L1/GAPDH
Ctrl
Ber
Pal

Figure 7